Toward a unified description of hadro- and photoproduction: S-wave π- and η-photoproduction amplitudes

Mark W. Paris and Ron L. Workman

Department of Physics, Data Analysis Center at the Center for Nuclear Studies, The George Washington University, Washington, D.C. 20052, USA

(Received 5 April 2010; revised manuscript received 12 July 2010; published 8 September 2010)

The Chew-Mandelstam (CM) parametrization, which has been used extensively in the two-body hadronic sector, is generalized in this exploratory paper to the electromagnetic sector by simultaneous fits to the π- and η-photoproduction S-wave multipole amplitudes for center-of-mass energies from the pion threshold through 1.61 GeV. We review the CM parametrization in detail to clarify the theoretical content of the SAID hadronic amplitude analysis and to place the proposed generalized SAID electromagnetic amplitudes in the context of earlier employed parametrized forms. The parametrization is unitary at the two-body level, which employs four hadronic channels and the γN electromagnetic channel. We compare the resulting fit to the MAID parametrization and find qualitative agreement; although, numerically, the solution is somewhat different. Applications of the extended parametrization to global fits of the photoproduction data and to global fits of the combined hadronic and photoproduction data are discussed.

DOI: 10.1103/PhysRevC.82.035202 PACS number(s): 13.60.−r, 11.55.Bq, 11.80.Et, 11.80.Gw

I. INTRODUCTION

Most of our knowledge of the excited baryons has come from fits to hadronic scattering data, in particular, pion-nucleon scattering, for which an accurate and nearly complete database exists that extends through and above the resonance region. Sufficient polarization observables exist to constitute complete measurements over a significant kinematic interval. The range of hadroproduction data, which includes $\pi N \to \pi N$, $\pi N \to \eta N$, $\pi N \to \omega N$, and other inelastic processes, which include, for example, strangeness production, have also been used to constrain theoretical models and phenomenological parametrizations of the scattering and reaction amplitudes.

Currently, however, a renaissance is underway in meson production and resonance physics with reaction data that issue from a number of precision electromagnetic facilities. Collaborative theoretical and phenomenological efforts have started to analyze these data in ways consistent with some subset of constraints imposed by quantum field theory upon the reaction amplitudes. The quality and quantity of data in electromagnetic-induced reactions are becoming sufficient to rival, and possibly surpass, the hadroproduction data. Since the electromagnetic reactions proceed mainly through the hadronic channels, the new data offer the possibility of backconstraining the hadronic amplitudes, conventionally determined only in fits to the hadroproduction data.

It is in this context that we have completed an exploratory study of the S-wave π- and η-photoproduction multipoles in the Chew-Mandelstam (CM) approach, related to the N/D representation, to the electromagnetic reaction amplitude. The novel concept, which provokes and permits this exploratory study, is the generalization of the CM approach to the electromagnetic sector. We have developed a new form for the amplitude that incorporates multichannel hadronic rescattering effects in a complete manner consistent with unitarity. The near-term objective is to develop a framework in which to analyze the hadro- and electroproduction reactions simultaneously in a global framework.

Recent experimental observations of the photoproduction of the η meson from the proton have yielded measurements of the unpolarized differential cross section [1–3] and photon beam asymmetry [4,5] of high precision. Forthcoming measurements from the CLAS Collaboration at Jefferson Laboratory [6] and Mainz [7] will rival, if not surpass, the precision of the existing measurements.

Several interesting features of η-meson physics motivate these measurements and their theoretical interpretation in various fields of nuclear physics, astrophysics, and particle physics. The possibility that the η-nucleon interaction may be attractive [8,9] suggests the existence of bound states of the η meson with nuclei. Certain resonances, the $S_{11}(1535)$ N^* resonance, in particular, are significantly coupled to the ηN channel, and the photoproduction of this final state provides an independent method to probe the isospin $T = \frac{1}{2}$ resonance spectrum and its couplings [10].

The strong interactions of the π and η mesons require multichannel descriptions that respect unitarity in the relevant channel space to obtain a realistic description of the data. The CM K-matrix approach [11–13] is an effective parametrization of the observed reaction data, since the elements of the CM K matrix may be assumed to be real if the couplings to neglected open channels are small.

Several relatively recent K-matrix analyses of the coupled πN, ηN, and γN channels [14–17] have been successful in obtaining reasonable parametrizations of the two-body partial-wave amplitudes [18]. The purpose of the present paper is to investigate the extent to which a description of the π photoproduction $E_{0+}^{1/2}(S_{11})$ amplitude and the modulus of the η photoproduction amplitude yields an η-photoproduction multipole with a resonant phase. Various calculations [16,19–21] indicate that the modulus of the η-photoproduction amplitude near threshold is fairly model independent, which is reproduced in a range of calculational models or schemes.

In the present paper, we take hadronic T-matrix elements as input, determined in realistic (χ squared per datum ~ 1) fits to data [22], as discussed in Secs. II–IV.

In Sec. II, we review the CM form [13] of the parametrization in some detail. The purpose of this review is to establish the theoretical considerations that motivate the amplitude parametrizations used in the SAID program, to place these amplitudes in the context of other hadronic amplitude parametrization schemes, and to lay the groundwork for future improvements. Section III gives the results for the fits to the isospin $T=\frac{1}{2}$ π-photoproduction amplitude E^{π}_{0+} and the modulus of the η-photoproduction amplitude E^{η}_{0+}. The conclusions are given in Sec. IV. We find, in this exploratory paper, an η-photoproduction multipole, which has a resonant shape, qualitatively similar to a Breit-Wigner form and similar to other calculations [19,21,23]. There is, however, significant deviation from the simple Breit-Wigner form.

II. CM PARAMETRIZATION

Previous work in the determination of the η-photoproduction amplitudes [14–16] has shown that an approach, which includes the coupling of the electromagnetic channel to the πN and ηN channels in the region of energies near the center-of-mass energy $W = 1535$ MeV, gives a reasonably good description of the data and a plausible form for the amplitudes. However, as our ultimate objective is the simultaneous parametrization of hadro- and photoproduction scattering and reaction observables, we will go beyond the two-channel treatment for this study of the E^{η}_{0+} multipole amplitude.

A. Unitarity constraint

The form of the CM parametrization, which we employ in this paper, follows as a consequence of the analytic structure imposed by the unitarity [24–28] of the S matrix in the physical region $W > m_i + m_t$, where W is the center-of-mass energy and m_i and m_t are the masses of the incident and target particles. By confining our attention to two-particle initial and final states, the S matrix is defined as

$$S_{\alpha\beta}(E) = \langle \mathbf{k}_\alpha \alpha | S | \mathbf{k}_\beta \beta\rangle \tag{1}$$

$$= \delta^{(3)}(\mathbf{k}_\alpha - \mathbf{k}_\beta)\delta_{\alpha\beta} + 2i\pi\delta(E_\alpha - E_\beta)\langle \mathbf{k}_\alpha \alpha | T | \mathbf{k}_\beta \beta\rangle, \tag{2}$$

where $\mathbf{k}_{\alpha,\beta}$ are the final and the initial relative momenta, respectively, $E = E_\alpha = E_\beta = W$ is the center-of-mass energy, and the labels α and β denote the particle species, spins, and internal quantum numbers, such as isospin. The initial and final energies E_β and E_α, respectively, are related to the on-shell relative momenta for channel α, $\bar{k}_\alpha$ as

$$W = E_{\alpha,1} + E_{\alpha,2}, \tag{3}$$

$$E_{\alpha,i} = \sqrt{\bar{k}^2_\alpha + m^2_{\alpha,i}}. \tag{4}$$

The on-shell relative momentum may be expressed in terms of the center-of-mass energy W as

$$\bar{k}_\alpha = \frac{1}{2W}\sqrt{W - m_{\alpha+}}\sqrt{W - m_{\alpha-}}\sqrt{W + m_{\alpha+}}\sqrt{W + m_{\alpha-}}, \tag{5}$$

with $m_{\alpha\pm} = m_{\alpha,1} \pm m_{\alpha,2}$.

The scattering operator S is unitary,

$$S^\dagger S = S S^\dagger = 1, \tag{6}$$

and, if we restrict our analysis to energies where just two-particle channels contribute, we obtain

$$\sum_\sigma \int d^3k_\sigma \langle \mathbf{k}_\alpha \alpha | S^\dagger | \mathbf{k}_\sigma \sigma\rangle \langle \mathbf{k}_\sigma \sigma | S | \mathbf{k}_\beta \beta\rangle = \delta^{(3)}(\mathbf{k}_\alpha - \mathbf{k}_\beta)\delta_{\alpha\beta}. \tag{7}$$

Substitution of Eq. (2) into the preceding relation yields the unitarity constraint on T:

$$T_{\alpha\beta} - T^\dagger_{\alpha\beta} = 2\pi i \sum_\sigma \int d^3k_\sigma T^\dagger_{\alpha\sigma}\delta(E_\alpha - E_\sigma)T_{\sigma\beta}. \tag{8}$$

By effecting the integration on $k_\sigma \equiv |\mathbf{k}_\sigma|$ gives

$$T_{\alpha\beta} - T^\dagger_{\alpha\beta} = 2i \sum_\sigma \int d\Omega_\sigma T^\dagger_{\alpha\sigma}\theta(W - m_{\sigma+})\rho_\sigma T_{\sigma\beta}, \tag{9}$$

where

$$\rho_\sigma(\bar{k}_\sigma) = \frac{\pi \bar{k}_\sigma E_{\sigma 1} E_{\sigma 2}}{W}. \tag{10}$$

The presence of the Heaviside step function $\theta(W - m_{\sigma+})$ is a consequence of the fact that, over the range of integration $k_\sigma > 0$, the argument of the δ function has a solution $E_\alpha - E_\sigma = 0$ only when $W > m_{\sigma+}$. Equation (9) implies discontinuities in the derivative of the imaginary part at each channel threshold $W = m_{\sigma+}$,

$$\frac{1}{2i}[T_{\alpha\beta} - T^*_{\alpha\beta}] = \mathrm{Im}\, T_{\alpha\beta} \tag{11}$$

$$= \sum_\sigma \int d\Omega_\sigma T^*_{\alpha\sigma}\theta(W - m_{\sigma+})\rho_\sigma T_{\sigma\beta}, \tag{12}$$

where we have assumed that because of the time-reversal invariance of the strong interaction $T_{\alpha\beta} = T_{\beta\alpha}$. The violation of the Cauchy-Riemann equations at the threshold indicates the presence of a branch point. We distinguish between the dynamical singularities at each threshold opening $m_{\sigma+}$ and kinematical singularities because of the presence of kinematical factors, such as $\bar{k}_\sigma$. The kinematical singularities are removed from the unitarity constraint by considering $T'_{\alpha\beta} = \sqrt{\rho_\alpha} T_{\alpha\beta}\sqrt{\rho_\beta}$.

We may transform to the partial-wave representation and write

$$T'_{\alpha\beta} - T'^*_{\alpha\beta} = 2i \sum_\sigma T'^*_{\alpha\sigma}\theta(W - m_{\sigma+})T'_{\sigma\beta}, \tag{13}$$

where the $T'_{\alpha\beta}$ now represent the partial-wave amplitudes. By casting this relation as a matrix equation,

$$\frac{1}{2i}[T' - T'^*] = T'^*\theta(W - M_+)T', \tag{14}$$

where $M_{+,\alpha\sigma} = m_{\sigma+}\delta_{\alpha\sigma}$ and by multiplying from the left by $[T'^{*}]^{-1}$ and from the right by T'^{-1} gives

$$\mathrm{Im}\, T'^{-1} = -\theta(W - M_+), \tag{15}$$

a diagonal matrix. Since this equation isolates the imaginary part of the inverse-T matrix, we write

$$\begin{aligned} T'^{-1} &= \mathrm{Re}\, T'^{-1} + i\mathrm{Im} T'^{-1}, &(16)\\ &= K'^{-1} - i\theta(W - M_+), &(17)\end{aligned}$$

where we have defined $\mathrm{Re}\, T'^{-1} = K'^{-1}$ and $K'_{\alpha\beta} = \sqrt{\rho_\alpha} K_{\alpha\beta}\sqrt{\rho_\beta}$. To multiply from one side by T' and the other by K' gives the Heitler integral equation [29,30]:

$$T' = K' + K' i\theta(W - M_+)T'. \tag{18}$$

This is the starting point for the CM parametrization of the reaction amplitude.

We emphasize that, in the physical region, the unitarity relation is satisfied by the imaginary part of T'^{-1}. Therefore, the Heitler K matrix is analytic, except for possible isolated poles [31] throughout the physical region [24,32]. This is apparent if we consider a dynamical equation of, for example, the Lippmann-Schwinger form

$$T = V + VG_0T, \tag{19}$$

$$G_0 = \mathcal{P}\frac{1}{E - H_0} - i\pi\delta(E - H_0). \tag{20}$$

Here, V is the interaction part of the full Hamiltonian $E = W$, H_0 is the free-particle Hamiltonian, and $\mathcal{P}$ denotes the Cauchy principal value prescription. Substitution of Eq. (20) into Eq. (19) gives $T = K + iK\delta(E - H_0)T$, where

$$K = V + V\mathcal{P}\frac{1}{E - H_0}K. \tag{21}$$

The Cauchy principal value prescription in this equation yields a kernel, which is completely continuous in the physical region. Therefore, the spectrum of the kernel possesses no eigenvalues in the continuum, and K is analytic (other than possible poles) there [33]. The K matrix may possess singularities in other regions of the complex energy plane. In fact, the interaction V possesses singularities in regions outside the physical region [34–36]. In particular, there is a branch point at some value $W < 0$. We intend to neglect singularities in the region Re $W < 0$ for the purposes of the present paper and avoid a detailed discussion of them here. A description is available in the literature [34–37]. Inclusion of singularities in the region Re $W < 0$ will be explored in subsequent investigations.

Therefore, the partial-wave amplitude is known to have the following singularities. There are branch points in the physical region at the channel-opening thresholds as in Eq. (9), branch points in the region $W < 0$, and possible poles consistent with causality [32,38]. An efficient parametrization that follows Ref. [37], which encodes these singularities, involves the factorization of the partial-wave amplitude. This is referred to as the N/D approach. We will use the N/D language to clarify the nature of the singularities of the T matrix, which are included and those neglected in our CM approach.

B. Relation to N/D approach

The N/D approach has been used to analyze a variety of reactions [37,39,40]. As our long-term objective is the generalization of the existing method used to parametrize the hadronic and electromagnetic amplitudes, here, we collect some of the relevant equations of the N/D approach. The T matrix is written in the factorized form

$$T(W) = D^{-1}(W)N(W), \tag{22}$$

where N and D are $N_{\mathrm{ch}} \times N_{\mathrm{ch}}$ arrays [28], where N_{ch} is the number of included two-body channels. This relation has been shown to be consistent with the requirement of time-reversal invariance in Ref. [41]. The relations,

$$\begin{aligned} &\mathrm{Im}\, D(W) = N(W)\,\mathrm{Im}\, T^{-1}(W), \quad W > m_i + m_t, &(23)\\ &\mathrm{Im}\, N(W) = 0, \quad W > m_i + m_t, &(24)\\ &\mathrm{Im}\, N(W) = D(W)\,\mathrm{Im}\, T(W), \quad W < 0, &(25)\\ &\mathrm{Im}\, D(W) = 0, \quad W < 0 &(26)\end{aligned}$$

give the essential content of the N/D approach. They state that the function D has branch points only in the physical $W > m_i + m_t$ region and that N has only unphysical $W < 0$ branch points. These relations determine the following dispersion relation (or Hilbert transform) representation for D:

$$\begin{aligned} D(W) = \sum_{i=1}^{n_p} D(W;W_i) - \frac{1}{\pi}\prod_{i=1}^{n_p}(W - W_i)\\ \times \int_{W_t}^{\infty} dW'\frac{N(W')\rho(W')}{(W' - W)\prod_j(W' - W_j)}, \end{aligned} \tag{27}$$

with n_p subtractions. Here, $D(W;W_i)$ is a polynomial of order n_p, $W \in \mathbb{C}$, and W_t is the lowest production threshold. Here, we show the polynomial ambiguity of the Hilbert transform explicitly to allow for the possibility that the parametrization includes several subtraction points.

By using the relation $T = ND^{-1}$ in the physical region, the numerator factor N can be shown to satisfy the integral equation,

$$\begin{aligned} N(W) = K\Bigg\{\sum_i D(W;W_i) - \frac{1}{\pi}\prod_{i=1}^{n_p}(W - W_i)\\ \times ⨍_{W_t}^{\infty} dW'\frac{N(W')\rho(W')}{(W' - W)\prod_j(W' - W_j)}\Bigg\}, \end{aligned} \tag{28}$$

where $⨍$ denotes the Cauchy principal value integral, and the Heitler K matrix K is defined by Eq. (18), with $K = \rho^{-1/2}K'\rho^{-1/2}$.

C. CM parametrization

The preceding discussion of unitarity and the N/D approach provide the context for our present parametrization. The CM parametrization developed here is similar to those of Refs. [11–13]. We consider Eq. (17) and rewrite it, by confining our attention to the S-wave multipole as

$$\begin{aligned} T^{-1} &= K^{-1} - i\tilde{\rho} &(29)\\ &= (K^{-1} + \mathrm{Re}\, C) - (\mathrm{Re}\, C + i\tilde{\rho})\\ &= \overline{K}^{-1} - C, &(30)\end{aligned}$$

where $\tilde{\rho} = \rho\theta(W - M_+)$ and Im$C = \tilde{\rho} = \theta(W - M_+)\rho$. The transition matrix is given in terms of the CM K matrix $\overline{K}$ by

$$T = \overline{K} + \overline{K}CT. \tag{31}$$

Equation (31) fixes our CM parametrization. In the language of Sec. II B, we have neglected the $W < 0$ branch points of N and made the approximation $N(W) = \overline{K}(W)$ an entire function. The CM function C_α is determined solely by the unitarity constraint Eq. (15), since Eq. (30) is equivalent to taking $D = 1 - \overline{K}C$. Then the CM function is given by a Cauchy integral over the discontinuity of C_α in the physical region,

$$C_\alpha(W) = \int_{W_t}^{\infty} \frac{dW'}{\pi} \frac{\rho_\alpha(W')}{W' - W} - \int_{W_t}^{\infty} \frac{dW'}{\pi} \frac{\rho_\alpha(W')}{W' - W_s}, \tag{32}$$

where we have made one subtraction $0 \leqslant W_s < W_t$. By defining $\overline{z}_\alpha = \frac{W - W_{t,\alpha}}{W - W_{s,\alpha}}$, we can rewrite Eq. (32) as

$$C_\alpha(W) = \int_0^1 \frac{dx}{\pi} \frac{\rho(x)}{x - \overline{z}_\alpha(W)}. \tag{33}$$

The relationship between the Heitler K matrix and the CM K matrix $\overline{K}$ is given by

$$K = \overline{K} + \overline{K}[\mathrm{Re}\, C]K. \tag{34}$$

This demonstrates a possible advantage of using the CM K matrix. If we consider a polynomial parametrization of a given CM K-matrix element,

$$\overline{K}_{\alpha\beta} = \sum_{n=0}^{n_{\alpha\beta}} c_{\alpha\beta,n} \overline{z}_{\alpha\beta}^n, \tag{35}$$

where $n_{\alpha\beta}$ are channel-dependent integers that control the order of the polynomial (polynomials typically less than fifth order are used) and $\overline{z}_{\alpha\beta}$ is a possibly channel-dependent linear function of the center-of-mass energy W, then, we see, by solving Eq. (34) for K,

$$K = \frac{1}{1 - \overline{K}[\mathrm{Re}\, C]}\overline{K}, \tag{36}$$

that poles may appear in the K matrix. Attempts to relate the K-matrix poles to resonances have been made [42–44]. Here, we simply point out that, although K-matrix poles are not simply related to T-matrix poles [31], Eq. (34) shows that one need not explicitly include pole terms in $\overline{K}$ to have poles in K. Parametrizing $\overline{K}(W) = N(W)$ as a polynomial, as noted, neglects singularities in the unphysical region $W < 0$ [45]. The branch points there and discontinuities across their associated branch cuts are determined by the production mechanisms [47] relevant for the reaction considered.

There are at least two reasons why polynomials may provide a reasonable starting point for a realistic parametrization of multichannel scattering and reaction amplitudes. The unitarity branch points, given their physical nature, largely determine the gross structure of the amplitudes in the physical region. This leads, in an obvious way, to the supposition that more distant singularities in the complex W plane associated, in particular, with the branch points in the unphysical region may be less important. Experience has also confirmed this to be true. The existing SAID parametrizations of πN elastic scattering [22], the $\pi N \to \eta N$ [10] reaction, π-photoproduction [48,49], electroproduction [50], and other reactions all reveal that a realistic description with χ^2 per datum in the range of 1–3 is possible with the polynomial approximation for $\overline{K}$.

III. RESULTS

The CM parametrization for the T matrix, described in Sec. II, has recently been applied [22] to a coupled-channel fit for the πN elastic scattering and the $\pi N \to \eta N$ reaction. It gives a realistic description of the data with χ^2 per datum better than any other parametrization or model to the best of our knowledge. The χ^2 per datum is shown in Table I against other parametrizations and model calculations for which we possess sufficient amplitude information to perform such an analysis [55]. The current SAID parametrization used in this fit is given as

$$T_{\alpha\beta} = \sum_\sigma [1 - \overline{K}C]^{-1}_{\alpha\sigma} \overline{K}_{\sigma\beta}, \tag{37}$$

where α, β, and σ are channel indices for the considered channels πN, $\pi\Delta$, ρN, and ηN. This parametrization has been discussed in Refs. [13,22,56]. Given the success of this approach in the hadronic two-body sector, the application to the study of meson photoproduction is warranted.

The central result of the current exploratory paper is to show that this form can be extended to include the electromagnetic channel,

$$T_{\alpha\gamma} = \sum_\sigma [1 - \overline{K}C]^{-1}_{\alpha\sigma} \overline{K}_{\sigma\gamma}, \tag{38}$$

where γ denotes the electromagnetic channel γN. Note that Eqs. (37) and (38) share the common factor $[1 - \overline{K}C]^{-1}_{\alpha\sigma}$, which encodes, at least qualitatively speaking, the hadronic channel-coupling (or rescattering) effects.

TABLE I. Normalized (left of each column pair) and unnormalized (right of each column pair) χ^2 per datum for the SP 06 [22] and FA 02 [51] solutions of SAID, KA 84 [52], EBAC [53], and GIESSEN [54]. The energy ranges of the four groups are from the threshold to 2.5, 2.9, 1.91, and 2.0 GeV, respectively [55].

	SP 06		FA 02		KA 84		EBAC		GIESSEN	
$\pi^+ p \to \pi^+ p$	2.0	6.1	2.1	8.8	5.0	24.9	13.1	23.7	10.5	17.7
$\pi^- p \to \pi^- p$	1.9	6.2	2.0	6.6	9.1	51.9	4.9	16.0	12.1	34.1
$\pi^- p \to \pi^0 n$	2.0	4.0	1.9	5.9	4.4	8.8	3.5	6.3	6.3	15.2
$\pi^- p \to \eta n$	2.5	9.6	2.5	10.5	–	–	–	–	–	–

The form Eq. (38) for photoproduction should be contrasted with that currently employed in the π-photoproduction studies of Refs. [15,48,49],

$$T_{\pi\gamma} = A(W)[1 + iT_{\pi\pi}(W)] + iB(W)T_{\pi\pi}(W), \quad (39)$$

where the structure functions $A(W)$ and $B(W)$ are parametrized as polynomials in the energy W, $T_{\pi\gamma} = T_{\pi N,\gamma N}$, and $T_{\pi\pi} = T_{\pi N,\pi N}$, and the factor $A(W)$ contains a contribution from tree-level Born diagrams. This satisfies the Watson theorem [57] [as does Eq. (38)] and is derived via the considerations discussed in Ref. [58]. While resulting in a realistic description of the data and being comparable, at least qualitatively, with other parametrizations such as MAID [23] for π photoproduction, it does not satisfy the full multichannel unitarity constraint imposed by Eq. (9). This deficiency led us to consider the form in Eq. (38), which manifestly satisfies the multichannel unitarity constraint Eq. (9).

The need to include the multichannel unitarity effects of Eq. (38) has also become apparent in difficulties faced in attempts to parametrize the η-photoproduction reaction by using forms [59] similar to Eq. (39). Forms of this type, used in fits to the η-photoproduction data alone, yielded an S-wave multipole without a clearly resonant shape, even while yielding fits to the observed data with realistic χ^2 per datum on the order of 2 to 4. An example of such a fit, which employs Eq. (39), is shown in Fig. 1. Near values of the center-of-mass energy $W \simeq 1535$, the amplitude in Fig. 1 is decidedly not resonant. This is also clear in the Argand plot of Fig. 2. Here, we have shown the comparison of the fit forms used in Ref. [59] (with energies marked by triangles). This difficulty was an early motivation for the present paper. Expectation of resonant behavior for η photoproduction $\gamma N \to \eta N$ in the S wave can be argued straightforwardly. For example, since the electromagnetic coupling to the πN channel is large, the $\gamma N \to \eta N$ reaction may proceed via the $\pi N \to \eta N$ amplitude of Fig. 3 or through direct resonance production. Therefore, we anticipate the hadronic subprocess will drive a significant resonant effect in the (isoscalar) electromagnetic transition.

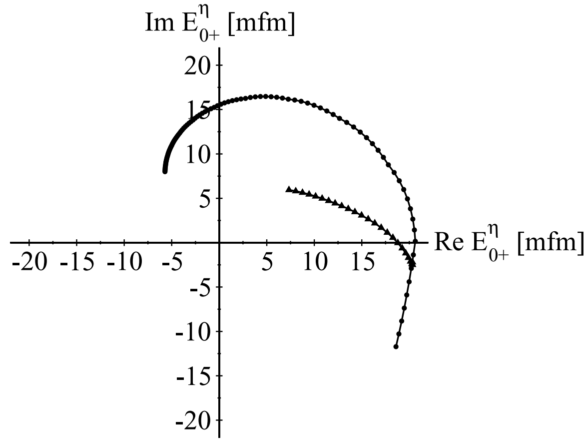

FIG. 2. Argand-plot comparison of the η-photoproduction S_{11} multipole amplitudes, versus Im E^{η}_{0+} plotted in the range 1490 MeV $\leqslant W \leqslant$ 1610 MeV of center-of-mass energy W with two fit forms. The curve with energies marked by triangles is another representation of the result for E^{η}_{0+} shown in Fig. 1, determined by using the parametrization of Eq. (39). The curve with energies marked by circles is another representation of the result for E^{η}_{0+}, shown in Fig. 5, determined by using the parametrization of Eq. (38). The curves span the same interval in energy but with different spacings. The first curve (triangles) is clearly nonresonant in the region shown, while the second curve (circles) clearly shows resonant behavior; the apex on the Argand diagram of the second curve occurs at precisely $W = 1535$ MeV.

Several other studies have determined that a resonant structure near $W \sim 1535$ MeV is consistent with the reaction data. These works include those in Refs. [16,19,21,23]. We should note that all of these works have assumed the S_{11} wave to be resonant, usually by including a Breit-Wigner or similar term explicitly into their formalism. We do not make this assumption in using Eq. (38).

In light of the study of Ref. [59] and the necessity of including the full multichannel unitarity for the purposes of obtaining a global description of the hadro- and photoproduction data, we have carried out an exploratory study to determine the

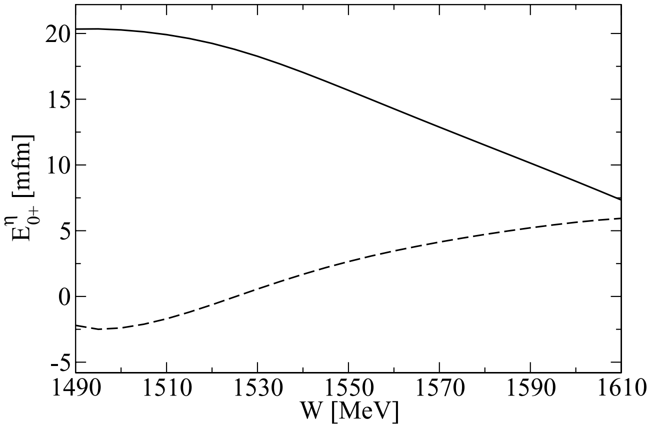

FIG. 1. The η-photoproduction S_{11} multipole amplitude E^{η}_{0+} versus the energy W fit by using the previously employed nonunitary form of Eq. (39). The behavior near $W \simeq 1535$ MeV is not resonant as can clearly be seen in Fig. 2.

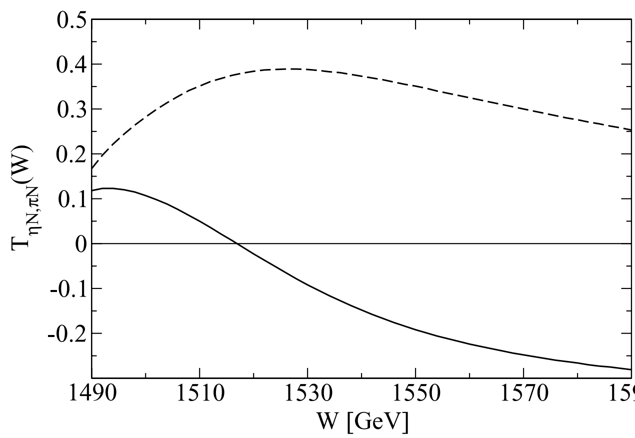

FIG. 3. The SAID S_{11} multipole for the $\pi N \to \eta N$ reaction as a function of energy W [10]. The solid (dashed) line is the real (imaginary) part of the amplitude.

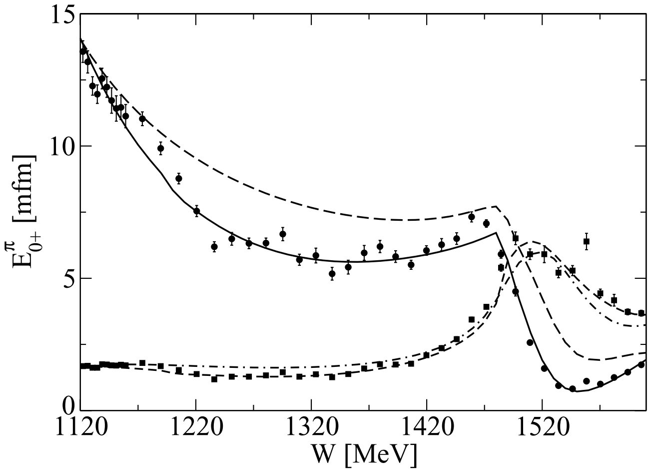

FIG. 4. Comparison of the SAID real (solid curve) and the imaginary (short-dashed curve) parts of the E^{π}_{0+} multipole amplitude with that of the MAID [60] real (long-dashed curve) and the imaginary (dot-dashed curve) parts. The amplitudes are plotted along with the real (circles) and the imaginary (squares) of the SAID single-energy solutions [60].

efficacy of doing such a fit within the CM parametrization Eq. (38). In the present paper, we perform a coupled-channel fit of the modulus $|E^{\eta}_{0+}(W)|$ and (the real and imaginary parts of) the existing SAID and MAID π-photoproduction amplitudes E^{π}_{0+} in the $S_{11}(1535)$ resonance region, compared in Fig. 4. The fit was carried out by taking the factor $[1-\overline{K}C]^{-1}_{\alpha\sigma}$ in Eq. (38), as determined in the the hadronic study of Ref. [22] and by adjusting the parameters of $\overline{K}_{\sigma\gamma}$ (discussed in detail in the following). The phase of the E^{η}_{0+} multipole in this paper gives a resonant wave and encourages us to continue with this approach, as discussed in Sec. IV.

The decision to fit the modulus $|E^{\eta}_{0+}|$ is based on empirical considerations. The MAID [23] parametrization and the model calculations in Refs. [16,19,21,61] agree at the few-percent level on the modulus of the low-energy η-photoproduction amplitude $|E^{\eta}_{0+}(W)|$. This is anticipated on the grounds that, in the $S_{11}(1535)$ resonance region, the differential cross section is largely angle independent and, therefore, is dominated by the S-wave production. It also indicates that the production is largely resonant, but we do not make this common assumption.

While the modulus $|E^{\eta}_{0+}|$ appears to be known at the level of a few percent, the π-photoproduction S_{11} amplitude is, surprisingly, not very well determined through different parametrizations. Figure 4 shows the SAID [22] and the MAID [23] results for E^{π}_{0+}. Given this discrepancy, we have also carried out the fit described earlier with the modulus $|E^{\eta}_{0+}|$ and the MAID parametrization.

A. Fit with SAID E^{π}_{0+}

Figure 5 shows the result of fitting the modulus $|E^{\eta}_{0+}|$ and the real and imaginary parts of the SAID E^{π}_{0+} multipole [48] by using an eight-parameter fit. The CM $\overline{K}$ matrix was assumed to have the form

$$\overline{K}_{\sigma\gamma}(W)=c_{\sigma\gamma,0}+c_{\sigma\gamma,1}\overline{z}_{\sigma\gamma}, \tag{40}$$

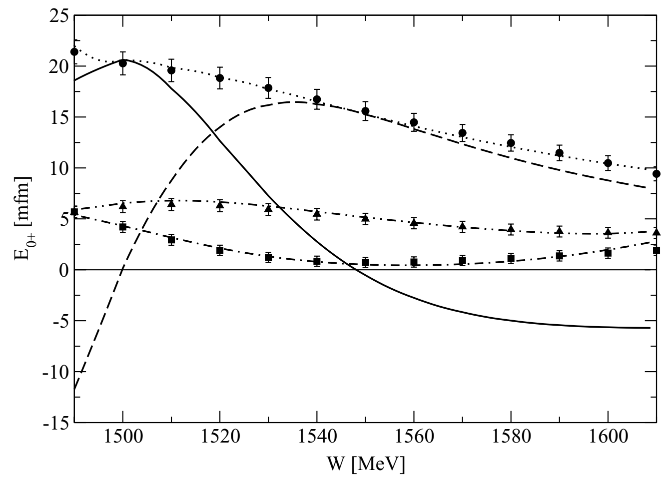

FIG. 5. The predicted values for the real (solid curve) and the imaginary (dashed curve) for E^{η}_{0+} versus the energy W. The modulus $|E^{\eta}_{0+}|$ (dotted curve), the real (dot-dashed curve), and the imaginary (double dot-dashed curve) parts of the π-photoproduction E^{π}_{0+} were fit to pseudodata generated from the SAID solution [48] with the parametrized form Eq. (38) by using eight parameters (see text).

by taking $n_{\alpha\beta}=1$ in Eq. (35), for α and β by taking values in the set of four channels πN, $\pi\Delta$, ρN, and ηN. The energy variable $\overline{z}_{\alpha\beta}$ is

$$\overline{z}_{\alpha\beta}=W-W_{t,\alpha}, \tag{41}$$

where the threshold masses $W_{t,\alpha}$ are $m_\pi+m_N$, $2m_\pi+m_N$, $2m_\pi+m_N$, and $m_\eta+m_N$ for $\alpha=\pi N$, $\pi\Delta$, ρN, and ηN, respectively, and $W_{t,\alpha}$ is taken to be the lower of the thresholds for channels α and β. The eight parameters were varied in the fit to a total of 113 pseudodata points, which include the modulus $|E^{\eta}_{0+}|$ over the energy range 1490 MeV $\leqslant W \leqslant$ 1610 MeV and the amplitude E^{π}_{0+} over the energy range 1120 MeV $\leqslant W \leqslant$

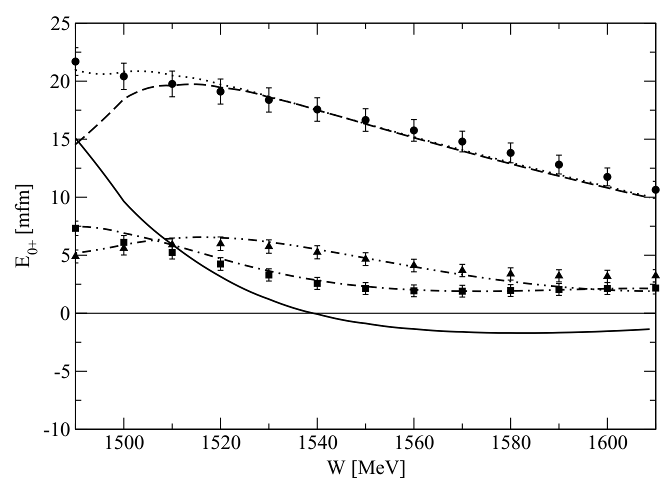

FIG. 6. The predicted values for the real (solid curve) and the imaginary (dashed curve) for E^{η}_{0+} versus the energy W. The modulus $|E^{\eta}_{0+}|$ (dotted curve), the real (dot-dashed curve), and the imaginary (double dot-dashed curve) parts of the π photoproduction E^{π}_{0+} were fit to pseudodata generated from the MAID solution [60] with the parametrized form Eq. (38) by using seven parameters (see text).

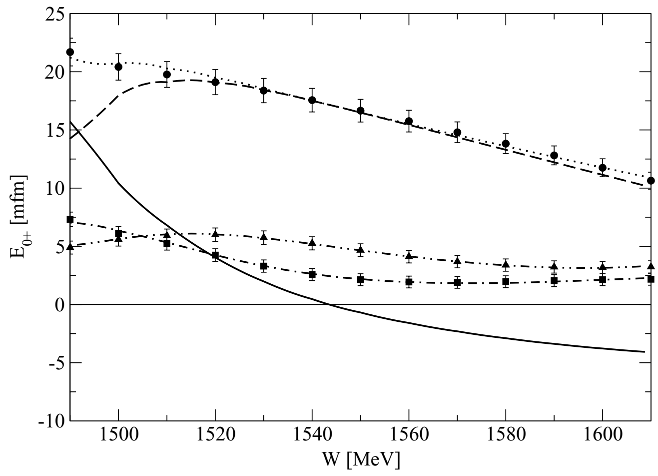

FIG. 7. The predicted values for the real (solid curve) and imaginary (dashed curve) for E^{η}_{0+} versus the energy W. The modulus $|E^{\eta}_{0+}|$ (dotted curve), the real (dot-dashed curve), and the imaginary (double dot-dashed curve) parts of the π photoproduction E^{π}_{0+} were fit to pseudodata generated from the MAID solution [60] with the parametrized form Eq. (38) by using 14 parameters (see text).

1610. The χ^2 per datum over for the fits to the pseudodata, generated with the SAID interactive code facility [62], were less than one in all of the fits made in this paper, which include those in the region 1120 MeV $\leqslant W \leqslant$ 1490 MeV, which are not displayed to keep the figures manageable and to focus attention on the $S_{11}(1535)$ resonance region. The pseudodata were assigned 5% errors in the fit.

B. Fit with MAID E^{π}_{0+}

The graphs in Figs. 6 and 7 used 7 and 14 parameters, respectively, to fit the $|E^{\eta}_{0+}|$ and E^{π}_{0+}amplitudes from MAID [23]. The seven-parameter fit in Fig. 6 is the minimal set of parameters needed to obtain a χ^2 per datum $\lesssim$1. The parameters used in Eq. (35) for this fit were $c_{\pi\gamma,n}$, $n = 0, 1, 2$, $c_{\rho\gamma,n}$, where $n = 0, 1$ and $c_{\eta\gamma,0}$ and $c_{\eta\gamma,1}$. The quality is

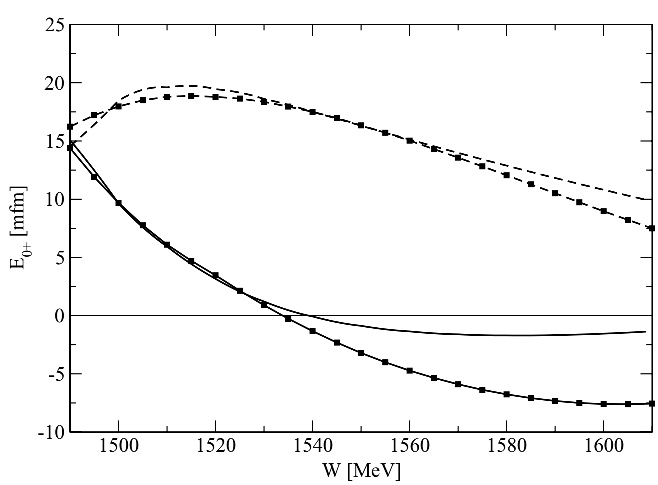

FIG. 8. The real (solid curves) and the imaginary (dashed curve) for E^{η}_{0+} from the seven-parameter fit in Fig. 6 compared with the η-MAID solution [23], marked by squares.

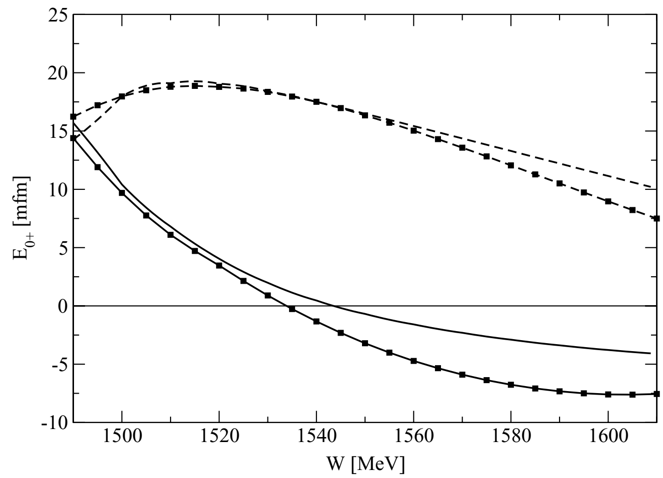

FIG. 9. The real (solid curves) and the imaginary (dashed curve) for E^{η}_{0+} from the 14-parameter fit in Fig. 7 compared with the η-MAID solution [23], marked by squares.

degraded at the higher-energy end of the fit region for the imaginary part of E^{π}_{0+}. Nearly perfect agreement is obtained if we use a 14-parameter form for $\overline{K}_{\sigma\gamma}$. The parameters used in Eq. (35) for this fit were $c_{\pi\gamma,n}, c_{\Delta\gamma,n}, c_{\rho\gamma,n}$, where $n = 0, 1, 2, 3$ and $c_{\eta\gamma,0}$ and $c_{\eta\gamma,1}$.

Note, from Figs. 8 and 9, that the fit, which gives the better representation of the MAID E^{π}_{0+} amplitude is similarly closer to the MAID E^{η}_{0+} result. This is somewhat surprising perhaps, since although the MAID pion and the η photoproduction use the same pole positions in both amplitudes, these parametrizations are not constrained by unitarity.

IV. CONCLUSION AND ONGOING WORK

We reviewed the implication of unitarity on the analytic structure of the single-meson production scattering and reaction amplitudes. The nonanalyticities in the regions $W > 0$ and $W < 0$, the right- and left-hand cuts, respectively, were demonstrated to be properly accounted for by the N/D approach. We related the CM K-matrix parametrization to the N/D approach by showing that the parametrization of the $\overline{K}$ matrix neglects the effects of the distant left-hand cut. The purpose of this review is to place the long-used SAID amplitudes in the context of other hadronic amplitude parametrization schemes and to lay the groundwork for future improvements to the existing parametrization forms.

By using the CM K matrix $\overline{K}$, we performed a simultaneous coupled-channel fit of the η photoproduction S_{11} multipole modulus $|E^{\eta}_{0+}|$ and the π-photoproduction amplitude E^{π}_{0+}. The parametrization was restricted only to the CM K-matrix elements $\overline{K}_{\sigma\gamma}$ in Eq. (38), while the $[1 - \overline{K}C]^{-1}$ factors were taken from the existing SAID fits to the hadronic data. The anticipated resonant structure for the phase of the E^{η}_{0+} multipole was demonstrated in fits to SAID amplitudes.

The results of the exploratory study indicate that this is a reasonable approach toward the objective of determining a complete set of scattering and reaction amplitudes for $\pi N \to \pi N$, $\pi N \to \eta N$, $\gamma N \to \pi N$, and $\gamma N \to \eta N$

processes in a multichannel unitary formalism. The first stage in this procedure, which demonstrates that coupled-channel simultaneous fits of the π- and the η-photoproduction reactions for a single partial wave (S_{11}) is possible, has been completed. The next phase consists of a fit to the π-photoproduction reaction observables. By following this, a simultaneous fit to the reaction observables for the π- and the η-photoproduction reactions will be performed. As a practical matter, these two phases will be completed by using the $[1-\overline{K}C]^{-1}$ rescattering factors determined in separate fits to the hadronic scattering and reaction data. The final phase of the study will be a simultaneous fit to both the hadronic and the electromagnetic scattering and reaction observables and will constitute, at least for two-body unitarity, a global description of the hadro- and photoproduction amplitudes.

ACKNOWLEDGMENTS

We thank R. Arndt without whom this work would not be possible. This work was supported in part by the US Department of Energy Grant No. DE-FG02-99ER41110. We thank the Department of Energy's Institute for Nuclear Theory at the University of Washington for its hospitality and the Department of Energy for partial support during the initiation of this work.

[1] V. Crede *et al.* (CB-ELSA Collaboration), Phys. Rev. Lett. **94**, 012004 (2005).
[2] T. Nakabayashi *et al.*, Phys. Rev. C **74**, 035202 (2006).
[3] M. Williams *et al.* (CLAS Collaboration), Phys. Rev. C **80**, 045213 (2009).
[4] J. Ajaka *et al.*, Phys. Rev. Lett. **81**, 1797 (1998).
[5] D. Elsner *et al.* (CBELSA Collaboration), Eur. Phys. J. A **33**, 147 (2007).
[6] M. Dugger *et al.* (CLAS Collaboration), (2004) [http://www.jlab.org/exp_prog/proposals/05/PR05-012.ps].
[7] J. C. McGeorge *et al.*, Eur. Phys. J. A **37**, 129 (2008).
[8] W. K. Cheng, T. T. S. Kuo, and G. L. Li, Phys. Lett. B **195**, 515 (1987).
[9] Q. Haider and L. C. Liu, Acta Phys. Polon. Suppl. **2**, 121 (2009).
[10] S. Prakhov *et al.*, Phys. Rev. C **72**, 015203 (2005).
[11] J. L. Basdevant and E. L. Berger, Phys. Rev. D **19**, 239 (1979).
[12] B. J. Edwards and G. H. Thomas, Phys. Rev. D **22**, 2772 (1980).
[13] R. A. Arndt, J. M. Ford, and L. D. Roper, Phys. Rev. D **32**, 1085 (1985).
[14] A. M. Green and S. Wycech, Phys. Rev. C **55**, 2167 (1997).
[15] R. A. Arndt, A. M. Green, R. L. Workman, and S. Wycech, Phys. Rev. C **58**, 3636 (1998).
[16] A. M. Green and S. Wycech, Phys. Rev. C **60**, 035208 (1999).
[17] V. Crede *et al.* (CBELSA/TAPS Collaboration), Phys. Rev. C **80**, 055202 (2009).
[18] The K-matrix approach of Refs. [14–16] include contributions to the hadronic T matrix, which represent the $\pi\pi N$ channel, although the three-body cut is not accounted for properly.
[19] N. Kaiser, T. Waas, and W. Weise, Nucl. Phys. A **612**, 297 (1997).
[20] L. Tiator, G. Knochlein, and C. Bennhold, PiN Newslett. **14**, 70 (1998).
[21] I. G. Aznauryan, Phys. Rev. C **68**, 065204 (2003).
[22] R. A. Arndt, W. J. Briscoe, I. I. Strakovsky, and R. L. Workman, Phys. Rev. C **74**, 045205 (2006).
[23] W.-T. Chiang, S.-N. Yang, L. Tiator, and D. Drechsel, Nucl. Phys. A **700**, 429 (2002).
[24] W. Zimmerman, Nuovo Cimento **21**, 249 (1961).
[25] R. J. Eden, Proc. R. Soc. London, Ser. A **210**, 388 (1952).
[26] J. C. Polkinghorne, Nuovo Cimento **23**, 360 (1962).
[27] J. B. Boyling, Nuovo Cimento **33**, 1356 (1964).
[28] J. D. Bjorken, Phys. Rev. Lett. **4**, 473 (1960).
[29] W. Heitler, Math. Proc. Camb. Phil. Soc. **37**, 291 (1941).
[30] M. L. Goldberger and K. M. Watson, *Collision Theory* (Wiley, New York, 1964).
[31] R. L. Workman, R. A. Arndt, and M. W. Paris, Phys. Rev. C **79**, 038201 (2009).
[32] R. J. Eden, P. V. Landshoff, D. I. Olive, and J. C. Polkinghorne, *The Analytic S-matrix* (Cambridge University Press, Cambridge, U.K., 1966), pp. 231–232.
[33] S. Weinberg, Phys. Rev. **133**, B232 (1964).
[34] S. Mandelstam, Phys. Rev. **112**, 1344 (1958).
[35] S. C. Frautschi and J. D. Walecka, Phys. Rev. **120**, 1486 (1960).
[36] W. R. Frazer and J. R. Fulco, Phys. Rev. **119**, 1420 (1960).
[37] G. F. Chew and S. Mandelstam, Phys. Rev. **119**, 467 (1960).
[38] N. M. Queen and G. Violini, *Dispersion Theory in High-Energy Physics* (Wiley, New York, 1974), pp. 13–14.
[39] R. A. Arndt, Phys. Rev. **165**, 1834 (1968).
[40] A. O. Barut, *The Theory of the Scattering Matrix* (Macmillan, New York, 1967), pp. 211–222.
[41] J. D. Bjorken and M. Nauenberg, Phys. Rev. **121**, 1250 (1961).
[42] A. D. Martin and T. D. Spearman, *Elementary Particle Theory* (North-Holland, Amsterdam, 1970).
[43] R. M. Davidson and N. C. Mukhopadhyay, Phys. Rev. D **42**, 20 (1990).
[44] S. Ceci, A. Svarc, B. Zauner, M. Manley, and S. Capstick, Phys. Lett. B **659**, 228 (2008).
[45] We note that the current parametrization neglects the constraints of chiral symmetry near the threshold and in the unphysical region. Therefore, the Adler zero [46] is, too, neglected.
[46] S. L. Adler, Phys. Rev. **137**, B1022 (1965).
[47] O. Babelon, J. L. Basdevant, D. Caillerie, and G. Mennessier, Nucl. Phys. B **113**, 445 (1976).
[48] R. A. Arndt, R. L. Workman, Z. Li, and L. D. Roper, Phys. Rev. C **42**, 1853 (1990).
[49] R. A. Arndt, R. L. Workman, Z. Li, and L. D. Roper, Phys. Rev. C **42**, 1864 (1990).
[50] R. A. Arndt, I. I. Strakovsky, and R. L. Workman, PiN Newslett. **16**, 150 (2002).
[51] R. A. Arndt, W. J. Briscoe, I. I. Strakovsky, R. L. Workman, and M. M. Pavan, Phys. Rev. C **69**, 035213 (2004).
[52] R. Koch, Z. Phys. C **29**, 597 (1985).
[53] B. Julia-Diaz, T. S. H. Lee, A. Matsuyama, and T. Sato, Phys. Rev. C **76**, 065201 (2007).
[54] V. Shklyar, H. Lenske, U. Mosel, and G. Penner, Phys. Rev. C **71**, 055206 (2005).

[55] The χ^2-per-datum analysis presented in Table I includes results for groups that have provided amplitudes in a manner, which allows the reconstruction of observables at arbitrary angle and energy.
[56] R. A. Arndt, I. I. Strakovsky, R. L. Workman, and M. M. Pavan, Phys. Rev. C **52**, 2120 (1995).
[57] K. M. Watson, Phys. Rev. **88**, 1163 (1952).
[58] R. L. Workman, Phys. Rev. C **74**, 055207 (2006).
[59] R. A. Arndt (private communication).
[60] D. Drechsel, S. S. Kamalov, and L. Tiator, Eur. Phys. J. A **34**, 69 (2007).
[61] F. Tabakin, S. A. Dytman, and A. S. Rosenthal, presented at the *Topical Conference on Excited Baryons Troy, NY, 1988* (World Scientific, Teaneck, NJ, 1988), pp. 168–198.
[62] The SAID interactive suite of codes is available by secure shell interface via: ssh -C -X said@said.phys.gwu.edu.